REVIEW OF SOLAR CELL TEMPERATURE COEFFICIENTS FOR SPACE

Geoffrey A. Landis
NYMA, Inc.
Brook Park, Ohio

INTRODUCTION

Energy conversion efficiency is an important parameter for solar cells, and well reported in the literature. However, solar cells heat up when in sunlight, and the efficiency decreases. The temperature coefficient of the conversion efficiency is thus also extremely important, especially in mission modeling, but is much less well reported. It is of value to have a table which compiles into a single document values of temperature coefficient reported in the literature.

In addition to modeling performance of solar cells in Earth orbit, where operating temperatures may range from about 20°C to as high as 85° C, it is of interest to model solar cells for several other recently proposed missions. These include use for the surface of Mars, for solar electric propulsion missions that may range from Venus to the Asteroid belt, and for laser-photovoltaic power that may involve laser intensities equivalent several suns. For all of these applications, variations in operating temperature away from the nominal test conditions result in a significant changes in operating performance.

In general the efficiency change with temperature is non-linear, however, in the range from negative 100 °C through room temperature to a few hundred degrees C, efficiency is usually quite well modeled as a linear function of temperature (except for a few unusual cell types, such as amorphous silicon, and for extremely low bandgap cells, such as InGaAs). Typical curves of efficiency versus temperature are shown in figure 1, from Reference [9].

TEMPERATURE COEFFICIENTS

This is a compilation of data reported in the literature on a variety of cell types. Not all literature values were reported. Some of the literature is ambiguous (for example, not listing whether reported values are normalized), or lacks required information (for example, reporting power variation in mW/°C without reporting cell power, or reporting I_{sc} variation without listing cell area). This compilation is also biased toward more recent cell types and cell types currently in production, and data on several old cell designs no longer in use has been left out.

These parameters are reported in terms of the normalized coefficients, that is, the fractional change in value per degree Celsius, $1/\eta \; d\eta/dT$. Clearly, the same coefficients apply to both efficiency and power, $1/\eta \; d\eta/dT = 1/P \; dP/dT$. A negative coefficient indicates a decrease in efficiency as temperature rises. Thus, given the efficiency at the nominal measurement temperature T_o, the efficiency at T is:

$$\eta(T) = \eta(T_o) \; [1+(1/\eta \; d\eta/dT)(T_o - T)] \qquad (1)$$

The temperature coefficient can be resolved into the sum of the variations of the open circuit voltage, V_{oc}, the short circuit current, J_{sc}, and the fill factor, FF:

$$1/\eta \; d\eta/dT = 1/V_{oc} \; dV_{oc}/dT + 1/J_{sc} \; dJ_{sc}/dT + 1/FF \; dFF/dT \qquad (2)$$

The V_{oc} variation contributes the majority of the change in efficiency. The V_{oc} and FF variations can be found in the references and are not tabulated here. The short circuit current temperature coefficient, $1/J_{sc} \; dJ_{sc}/dT \; (= 1/I_{sc} \; dI_{sc}/dT)$ is reported, for reasons discussed below.
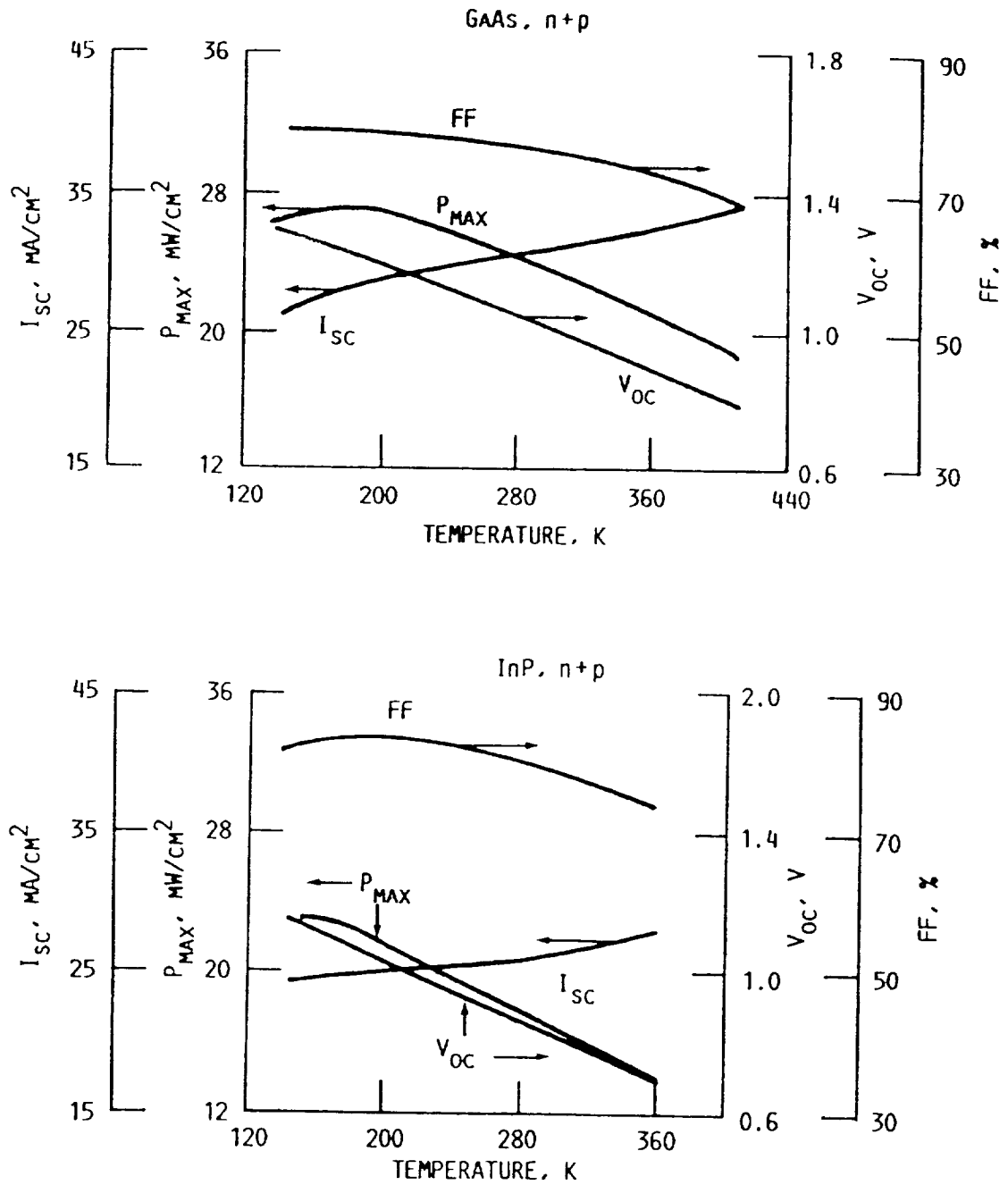
Figure 1

Variation of maximum power (P_{max}) and Voc, Isc, and fill factor with temperature for gallium arsenide solar cell (top) and indium phosphide solar cell (bottom) (data from Weinberg et al. [9], used with permission of the author).

The wide variability in the quoted values of the J_{sc} temperature coefficient for cells of the same general type deserves discussion. The values differ not only from each other, but from the actual value measured under space conditions. This can be seen, for example, in a comparison of temperature coefficients measured using simulated sunlight compared with measurements made in space on the NTS-1 mission [table 4-12 of reference 32, reproduced as figure 2]. The temperature coefficients of voltage match to well within the error bars of the measurement. Measured temperature coefficients of J_{sc}, on the other hand, are incorrect by an average of 340 percent.

Variation of short circuit current with temperature is primarily due to the change in bandgap energy with temperature. As the cell heats up, the bandgap decreases, and hence the cell responds further into the infrared portion of the spectrum. Hence, the J_{sc} variation term is roughly proportional to the incident spectral intensity at wavelengths near the band edge. Solar cells are not typically tested under actual sun illumination, however, but under a solar simulator, often a Xenon lamp. While a Xenon lamp has a spectrum that approximates that of the solar spectrum on the average, the intensity does not duplicate the solar spectrum in detail [31]. This is shown in figure 3. In particular, the spectral intensity near the semiconductor band edge (the range from about 800 to 1100 nm for silicon and GaAs cells) is significantly different from that of the sun, and in general different simulators (even of the same type) will have differences in the detailed structure. Thus, the variability of J_{sc} temperature coefficient is due to variations in the solar simulator, and not differences in the cells.

Measurements of J_{sc} temperature coefficient made with simulated sunlight cannot be trusted. Fortunately, the J_{sc} variation accounts for only about 10-20 percent of the efficiency variation. For greatest accuracy, it is suggested that the measured $1/J_{sc} \, dJ_{sc}/dT$ term should be subtracted from the normalized power temperature coefficient to cancel this variation, and a calculated value appropriate to the cell material should be substituted. For Si and GaAs cells, use of values from flight experiments (last lines of tables 1 and 2) are suggested.

Tables 1-2 give the compiled values of temperature coefficients from the solar cell literature, along with the temperature range of the measurement and the cell efficiency when listed, for silicon and GaAs space solar cells. The first three values in the list show current production cells for space. Table 3 compiles temperature coefficient data for various emerging materials not yet being used for space power. Table 4 shows values for low-bandgap TPV cells under 1500° blackbody illumination. Note that since 1500° blackbody radiation contains considerably higher amounts of infrared than the solar spectrum, the J_{sc} temperature coefficient is much higher than under solar spectrum illumination.

As expected, the temperature coefficients varies with the bandgap of the material, with the highest temperature dependence shown by the materials with lowest bandgaps. For comparison, table 5 shows the theoretical values of temperature coefficient for idealized GaAs, Si, and Ge cells [24]. The efficiencies of these idealized cells are higher than that of those achieved today, and hence the temperature coefficients are slightly lower. However, the theoretical values for efficiency coefficient agree rather well with the measured values for the GaAs and the Ge cells, as well as for the best of the silicon cells. For reasons discussed above, the short-circuit current coefficients do not agree very well.

The emphasis here is for space operation (Air Mass Zero spectrum). However, since the Voc and FF coefficients are not dependent on spectrum, most of this data is also usable for terrestrial calculations.

Reference [24] discusses the theoretical basis for the variation of performance with temperature. The largest term in the temperature dependence is the voltage term, which is:

$$dV_{oc}/dT = (V_{oc} - Eg/q)/T - 3k/q - d(Eg/q)/dT + kT/q(1/J_{sc} \, dJ_{sc}/dT) \qquad (3)$$

Exp. No.	$\dfrac{dV_{oc}}{dT}$ (mV/°C)		$\dfrac{dI_{sc}}{dT}$ (mA/°C/4 cm²)	
	Ground Measurement	Space Measurement	Ground Measurement	Space Measurement
1	2.114	2.139 ± .178	.045	.197 ± .064
2	2.082	2.144 ± .113	.058	.213 ± .137
4	1.941	1.871 ± .149	.096	.271 ± .093
5	2.191	2.098 ± .117	.046	.139 ± .047
6	2.082	1.989 ± .140	.058	.170 ± .041
7	1.973	2.089 ± .149	.076	.231 ± .055
8	2.082	2.098 ± .127	.058	.225 ± .061

Figure 2

Measure of voltage and current temperature coefficients for 8 silicon solar cell experiments flown on NTS-1 satellite, comparing measurements made on the ground with those made in space [from ref. 32].
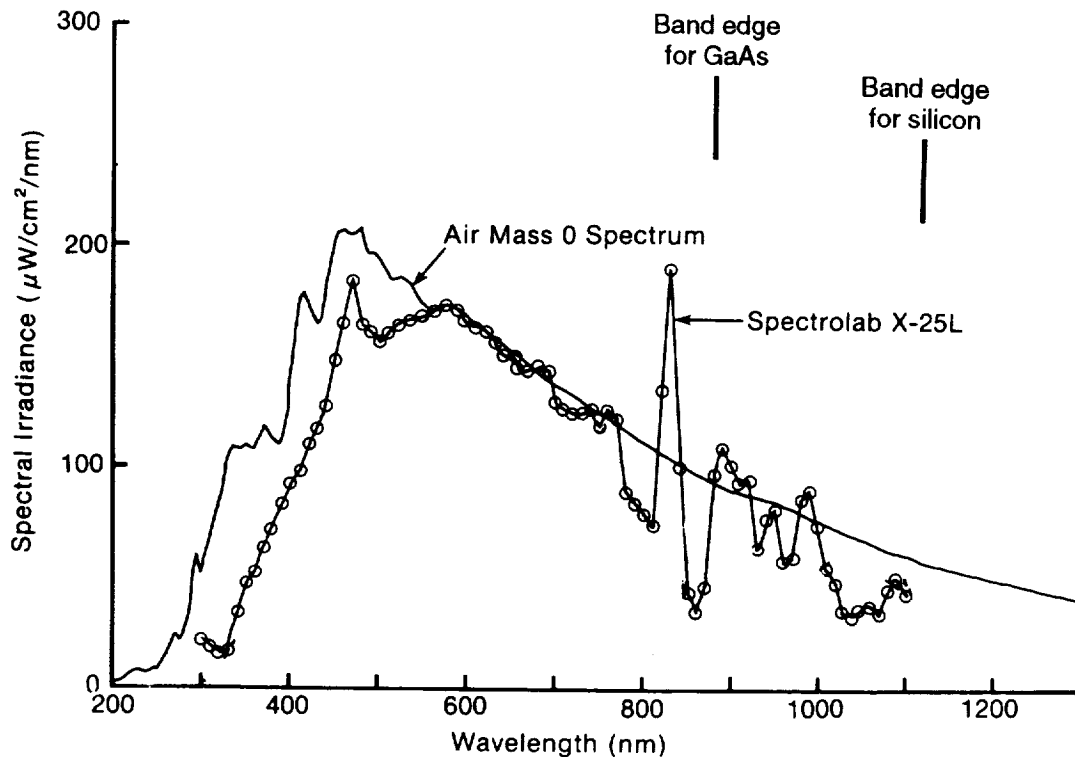
SOURCE: Seaman et al. 1980

Figure 3

Spectral comparison of Spectrolab X-25 Xenon-Arc Solar Simulator with AM0 solar spectrum

where Eg/q is the bandgap in volts, T the temperature, and k/q the thermal voltage, equal to 0.086 mV/°C. Parameters to calculate the bandgap change with voltage for GaAs, Si, and Ge are given in [24], and for InP in [16].

The largest contribution comes from the first term, proportional to the difference between the bandgap and the open circuit voltage. Temperature coefficient thus decreases nearly linearly as voltage increases. Since higher efficiency cells typically have higher open circuit voltages, higher efficiency cells tend to have lower temperature coefficients than low efficiency cells of the same material. This can be clearly seen in table 1.

Temperature coefficient is rarely considered as a design parameter for solar cells. From the standpoint of temperature coefficient, increasing open circuit voltage, even at the expense of decreases in other cell parameters (for example, by increasing base doping of the cell) may result in higher power under actual space operating conditions.

Since open circuit voltage increases logarithmically with short circuit current, temperature coefficient decreases as the log of the intensity. This is shown in the graph of temperature coefficient versus intensity for GaAs solar cells [from Swartz and Hart, [11]]. For cells with low bandgap, such as Ge, the fractional rise in voltage is higher, and thus the decrease in the coefficient with intensity larger. Since temperature coefficient is a function of illumination level, these tables do not report temperature coefficients for concentrator solar cells [33-36].

At low temperature, the linear approximation is less valid. The increase in efficiency as temperature decreases tends to level off, reaching a plateau typically typically around -80°C for silicon cells [see figures 4-57 through 4-60 of reference 32]. At low illumination intensity and low temperature ("LILT" conditions), some solar cells are subject to additional degradation in performance. References [39], [40], and [41] discuss operation of silicon solar cells at low temperatures and low intensity.

OPERATING TEMPERATURE AND EFFICIENCY

Operating temperature can be calculated from equating the power incident on the array, P_{in}, with the power produced plus that radiated away, P_{out}. Here

$$P_{in} = \alpha_{solar} P_{sun} + \text{albedo } P_{albedo} + \alpha_{thermal} P_{thermal} \qquad (4)$$

and

$$P_{out} = \eta(T)P_{sun} + \varepsilon_{front} \sigma T^4 + \varepsilon_{rear} \sigma T^4 \qquad (5)$$

where T is in degrees Kelvin and σ is the Stefan-Boltzmann constant, $5.67 \cdot 10^{-8}$ W/m²-°K⁴. For the case of a laser-illuminated array there are additional terms corresponding to the laser incident power and the laser conversion efficiency [47]. Equating these and inserting η as a linear function of T results in a fourth-order equation, which is typically solved by Newton's method.

Note that in calculating temperatures in low Earth orbit, the contribution of sunlight reflected from the Earth ("albedo") and thermal infrared radiated from the Earth must be accounted for. The Earth's albedo varies with cloud cover and season. Average values for P_{albedo} are quoted as "up to 30%" [31], "about 0.3" [28], and 0.35 [1]. Note that albedo increases significantly at high latitudes in winter due to snow cover; this can be important for polar orbits. The worst (highest temperature) case is at orbital noon, when the albedo illumination is directly on the back of the array; for this reason, the rear-surface alpha is an important parameter and is listed in table 6 for the cases where it has been reported.

Thermal radiation also varies with position over the Earth and time of year. Typical thermal estimates use a thermal load in low Earth orbit (LEO) of about $P_{thermal}=0.17$ solar intensity [28,31], with

0.0030

0.0028

0.0026

0.0024

0.0022

0.0020

0.0018

1/η Δη/ΔT

GaAs planar cell

Theory:
Decrease in temperature coefficient proportiona
to voltage increase of 25 mV ln(Isc)

GaAs Concentrator
Cells

.1   1   10   100   1000

Intensity (AM0 Suns)

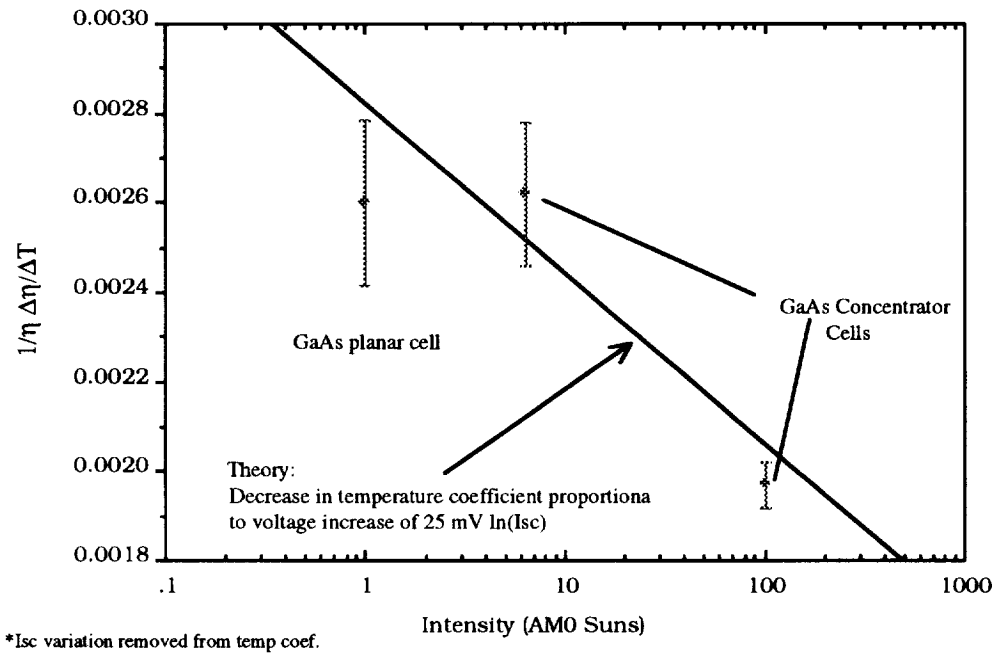*Isc variation removed from temp coef.

Figure 4

Normalized temperature coefficient (with Isc variation subtracted) of GaAs solar cells at various incident solar intensities. Line shows the expected variation if the only factor in temperature coeffient is the variation of Voc.

the spectrum of a 288 °K blackbody [31]. The absorption constant for thermal radiation $\alpha_{thermal}$ is the same as the thermal emissivity, ε, rather than the solar absorptivity α. Higher orbits reduce albedo and thermal loading proportionately to the solid angle subtended by the Earth. Hence (as can be seen in table 6) operating temperatures tend to be lower for GEO orbit (40,000 km altitude) than in LEO (800 km altitude).

The solar absorptivity, α, is a characteristic of the solar cell, subject to some modification by ultraviolet and/or infrared rejection filters on the coverglass. To reduce the solar absorptance, silicon cells may have back-surface reflectors ("BSR") to reflect unabsorbed infrared radiation back to space, or even gridded back contacts to transmit unused infrared directly through the array. Cells with textured surfaces have higher absorptance than cells with planar surfaces, and hence higher operating temperature. In the infrared, the glass cover on the solar array is typically opaque, and hence the thermal emittance ε is characteristic of the glass and independent of the cell type.

Table 6 gives some quoted values of the thermal parameters, α and ε, and also shows the calculated equilibrium operating temperatures in orbit for several cells.

Future cells may have advanced covers which more efficiently reflect undesired IR and UV radiation [43,44]. This can reduce the solar alpha for silicon cells to 0.75 for cells without back-surface reflectors or gridded back contacts [43], and to 0.72 to 0.79 [43, 44] for GaAs/Ge cells.

TEMPERATURE COEFFICIENTS FOR NON-SOLAR SPECTRA

There has recently been some interest in use of photovoltaic cells for converting laser radiation [45,46]. Equation 2 shows the components of the variation of efficiency with temperature. Of the three terms, only the J_{sc} term should depend on spectrum. Hence, the normalized temperature coefficient under laser illumination can be calculated from the efficiency and Jsc terms:

$$[1/\eta \ d\eta/dT]_{laser} = [1/\eta \ d\eta/dT]_{solar} - [1/J_{sc} \ dJ_{sc}/dT \ ]_{solar} + [1/J_{sc} \ dJ_{sc}/dT]_{laser} \quad (5)$$

Since the J_{sc} term typically contributes 10-20% of the efficiency variation with temperature, to single-digit accuracy the normalized efficiency temperature coefficient should be roughly the same for laser or solar illumination [47]. The V_{oc} term will have a slight dependence on spectrum because the laser wavelength may be chosen to be close to the cell spectral response maximum, and hence the current output for a given intensity input will be higher, resulting in a logarithmic increase in voltage and a slight decrease in temperature coefficient.

Under solar illumination the short circuit current increases with temperature. Under monochromatic illumination this may or may not be true. There are two regions of operation, depending on the wavelength of the laser and the shape of the cell spectral response (in A/W). The two regions are: (1) wavelength shorter than the spectral response peak, or (2) wavelength longer than the spectral response peak.

For wavelengths shorter than the spectral response peak, the semiconductor absorbs essentially all of the incident light, and this does not change as the bandgap changes with temperature. Changes in short circuit current are only due to changes in quantum efficiency, which should be close to unity for high efficiency cells. Since the number of incident photons is not dependent on the bandgap, the current is nearly independent of temperature, and the temperature coefficient of J_{sc} is near zero. Hence, for this region of operation, the monochromatic temperature coefficient can be approximated by subtracting the (solar) normalized J_{sc} temperature coefficient from the normalized efficiency coefficient.

For a cell operating at wavelengths longer than the peak of the spectral response this will not be

true. At long wavelengths the laser light is only weakly absorbed, and hence a small change in the bandgap will result in a large change in absorption. For such cells the J_{sc} will increase with temperature. This effect may be especially important in indirect bandgap materials, such as a silicon cell operated at 1.06μ. For such regimes of operation the change of absorption with temperature will be very significant, and the cell may even increase in efficiency with temperature.

The theoretical monochromatic J_{sc} temperature coefficient is:

$$[1/J_{sc} \; d J_{sc}/dT]_{laser} = \lambda/Eg \; (dQE/d\lambda)(dEg/dT) \qquad (6)$$

where QE is the cell quantum efficiency at the laser wavelength λ. The variation in bandgap energy with temperature for most materials, dEg/dT, can be found in the literature [16,24].

Solar cells can be used for spectra other than solar or laser. Wilt et al [47] discusses the temperature coefficient of 0.6 to 0.7 eV InGaAs cells under 1500 °C blackbody radiation; these results are shown in table 4. Note that, for these cells, the J_{sc} component of the temperature coefficients is a much larger component of the total. This is because of the low bandgap of the cell and the fact that the 1500° C blackbody has a large amount of its radiation in the infrared. The fact that these cells are operated under high intensity also means that the V_{oc} component of the temperature coefficient is somewhat reduced by the logarithmic dependence of V_{oc}.

For blackbody spectra, as for laser spectra, the temperature coefficient can be computed from the solar temperature coefficient by subtracting out the measured J_{sc} coefficient and replacing it with the J_{sc} coefficient for the spectrum desired.

CONCLUSIONS

The variation of solar conversion efficiency with temperature has been reviewed. The efficiency is assumed to be linear with temperature. This is correct for temperatures near 25° C for most cell types, but the behavior is nonlinear at extremely high and low temperatures. Typically the increase of efficiency with reduction of temperature flattens out below~200 °K. Also, at extremely high temperatures, the efficiency does not go to negative values, but levels off near zero. References 32 and 33 have data on (1967 vintage) silicon cells to temperatures down to 82 °K. The Design Handbook has data on later vintage silicon cells at low intensity and low temperatures [32].

Table 1: Silicon Cell Temperature Coefficients

The first cell listed, SSF gridded back, is the large-area silicon cell developed for the space station Freedom project. This, and the Applied Solar Energy Corporation (ASEC) Back Surface Field/Reflector (BSFR) and ASEC Back Surface Field (BSF) cells, may be taken typical of silicon cells currently used in flight, however, they are not significantly different in performance from the other silicon cells listed, with the exception of the last two.

The University of New South Wales (UNSW) cells are recently developed laboratory cells with improved open-circuit voltage and high efficiency. Cells of this design are not yet qualified for use in space.

Cell Type	Temp (°C)	η (28°C)	normalized temp. coefficients		Ref.
			$1/\eta \; d\eta/dT$ ($\times 10^{-3}$°C^{-1})	$1/J_{sc} \; dJ_{sc}/dT$ ($\times 10^{-3}$°C^{-1})	
SSF grid back	0-95	.13	-4.5		[1]
ASEC BSFR	28-60	.135-.148	-4.60		[2]
ASEC BSR	28-60	.125-.134	-4.45		[2]
2Ω High E.	0-140	.122	-4.62	+0.74	[3]
10Ω Helios	0-140	.116	-4.72	+0.59	[3]
10Ω BSF	0-75	.140	-5.0		[4]
2Ω K5	0-75	.136	-5.0		[4]
"Violet"	0-120	.14	-4.2	+0.65	[5]
CNR (text.)	10-70	.148	-4.35	+0.34	[5]
AEG 10Ω BSR		.122	-3.79	+1.14	[6]
UNSW MINP	5-60	.1870	-3.443	+0.650	[7]
UNSW PESC	5-60	.1907	-3.202	+0.650	[7]
NTS-1 space measurement (avg. 7 types)				+1.12	[32]

Table 2: GaAs Cell Temperature Coefficients

The ASEC GaAs/Ge cells listed on the first two lines can be taken as typical of cells that are currently flown in space.

Cell Type	Temp (°C)	η (28°C)	normalized temp. coefficients		Ref.
			$1/\eta \; d\eta/dT$ ($\times 10^{-3}$°C^{-1})	$1/J_{sc} \; dJ_{sc}/dT$ ($\times 10^{-3}$°C^{-1})	
ASEC GaAs/Ge	20-120	.174	-1.60	+0.830	[8]
ASEC GaAs/Ge	28-60	.18-.185	-2.23	+0.56	[2]
ASEC /GaAs	28-60	.18-.185	-2.32	+0.56	[2]
Spire /GaAs	10-80		-1.47	+0.246	[38]
Varian	60	.195	-2.2	+0.6	[9]
EEV LPE		.174	-1.90	+0.92	[10]
Hughes LPE	0-415	.157	-2.09	+1.1	[11]
French LPE	40-200	.212	-2.53		[12]
LPE	25-350	.156	-2.64	+0.37	[13]
DH	15-80		-2.74	+0.30	[14]
Hughes p/n	0-80	.164	-2.0	+0.714	[15]
LL n/p homo.	0-80	.166	-2.6	+0.71	[15]
Japan LPE p/n	0-100	.175	-2.10	+0.63	[37]
Varian	10-80	(high altitude test)		+0.508	[31]

393

Table 3: Temperature Coefficients from Cells of Other Materials

Cell Type	Temp (°C)	η (28°C)	normalized temp. coefficients $1/\eta \; d\eta/dT$ $(x10^{-3}°C^{-1})$	$1/J_{sc} \; dJ_{sc}/dT$ $(x10^{-3}°C^{-1})$	Ref.
1.7eV AlGaAs					
AlGaAs	15-80		-1.55	+0.95	[14]
1.93 eV AlGaAs					
Varian	25-96	(high altitude test)		+0.761	[31]
InP					
diffused (best)	60	.132	-3.45	+0.767	[16]
diffused (wrst)	60	.103	-3.56	+0.966	[16]
RPI	60	.136	-2.8	+0.8	[9]
MO-CVD	0-150	.195	-1.59	+0.890	[17]
ITO/InP	15-80		-3.80	+0.515	[14]
Ge					
RTI	20-80	.090	-10.1	+0.617	[18]
CuInSe₂					
Boeing CIS	-40-80	.087	-6.52		[19]
ISET CIS	-40-80	.088	-6.03		[19]
Boeing CIS	25	.08	-5.26	+0.43	[20]
CIS/CdZnS	15-80		-5.87	+0.260	[14]
CIS/CdS			-6.880	+0.057	[21]

Amorphous Si alloys Reported a-si cells have nonlinear response with temperature. Data reported here is for the region listed.

(single junction)					
Solarex	0-40	.066	-1.11*	+0.74	[19]
ECD a-si:H,F	15-80		-0.98 to -1.97*	0.83 to 0.95*	[14]
ECD aSiGe:H,F	15-80		-1.02 to -1.97*	1.01 to 1.36*	[14]

*nonlinear

(two junction)					
Fuji	22-60	.089-.10	2.0		[42]

GaAs/Ge Tandem					
low temp.*	35-100	.194	-2.85	+1.02	[22]
high temp.*	100-180	~.18	-2.0	+1.02	[22]
Spire	25-80	.189	-1.54	+0.94	[23]

[see also ref. 38]

*nonlinear

Table 4: Temperature Coefficients For Theromphotovoltaic (TPV) Cells under 1500°C blackbody radiation

Note that Jsc temperature coefficient will be much higher under 1500° blackbody radiation than under the solar illumination.

Cell Type	Temp (°C)	normalized temp. coefficients $1/\eta\ d\eta/dT$ (x10^{-3}°C^{-1})	$1/J_{sc}\ dJ_{sc}/dT$ (x10^{-3}°C^{-1})	Ref.
0.6eV InGaAs	30-70	-9.46	+3.04	[48]
0.66eV InGaAs	25-60	-10.12	+3.18	[48]
0.75eV InGaAs	30-60	-4.67	+2.00	[48]

note: the J_{sc} temperature coefficients for these cells are highly non-linear above 60°C.

Table 5: Calculated Values of Temperature Coefficients

These values are for theoretical cells with performance at or near the theoretical limit. Numbers are not representative of actual cells in use today.

Cell Material	Temp (°C)	η (28°C)	normalized temp. coefficients $1/\eta\ d\eta/dT$ (x10^{-3}°C^{-1})	$1/J_{sc}\ dJ_{sc}/dT$ (x10^{-3}°C^{-1})	Ref.
GaAs (calc.)	27	.277	-2.40	+0.34	[24]
Si (calc.)	27	.247	-3.27	+0.293	[24]
Ge (calc.)	27	.106	-9.53	+0.125	[24]

Table 6: Other Thermal Parameters

Cell	Front		Rear		Operating temp. (°C)		Orbit	Ref.
	α	ε	α	ε				
Silicon Cells/Arrays								
8x8 (SSF)	0.62	0.85	0.25	0.85	60	(η=13.5)	LEO	[1]
ASEC grd back	0.65					(η=14.2%)		[2]
ASEC BSR	0.68					(η=12.5-13.4%)		[2]
ASEC BSFR	0.72-0.74					(η=13.5-14.8%)		[2]
Si (HST) (BSFR Si)	0.75(cell) 0.54(array)	0.83	0.54	0.70	50-61		LEO	[25]
Silicon	0.80-0.84	0.81-0.84		0.81				[26]
Si K4, K6 (planar Si, gridded back)	0.63				23	(η=14%)	LEO	[4]
Si K5, K7 (textured Si, gridded back)	0.81				43	(η=14%)	LEO	[4]
Si BSFR	0.757	0.83	0.54	0.898	71	(η=8%)	LEO	
					44	(η=8%)	GEO	[27]
Si bifacial	0.66	0.83	0.57	0.78	57	(η=9%)	LEO	[27]
Si BSF 0.82	0.82			0.86	42	(η=14.2%)		[28]
Thin Si	0.72	0.86		0.86	27	(η=13.5%)		[28]
IR refl. Si	0.69	0.86		0.86	22	(η=14.4%)		[28]
IR transp. Si	0.67	0.86		0.86	21	(η=13.3%)		[28]
ASEC BST	0.65	0.88						[29]
Sharp BSFR Si	0.75	0.82		0.80	37	(η=14.3%)		[30]
textured cell (textured Si, no BSR)	0.93	0.77						[5]
textured cell (above, with conductive coated coverglass)	0.905	0.75						[5]
GaAs Cells								
ASEC /Ge	0.870					(η=18-18.5%)		[2]
ASEC/GaAs	0.83					(η=18-18.5%)		[2]
thin GaAs	0.82	0.86		0.86	36	(η=16.0%)	LEO	[28]
Sharp GaAs	0.86	0.82		0.80	45	(η=18.0%)		[30]
GaAs/Ge	0.88	0.80	0.20	0.85	84	polar 5600nm		[22]
GaAs	0.84	0.83	0.54	0.898	72	(η=9%)	LEO	
*					48	(η=9%)	GEO	[27]

REFERENCES

[1] J.F. Baumeister and S. Morren, Space Station Solar Thermal Analysis Presentation, 6/23/88, NASA Lewis.

[2] Applied Solar Energy Corporation; product data sheets (1993).

[3] Jet Propulsion Laboratory, *Solar Array Design Handbook, Volume II*, section 3.2 (Oct. 1976). Data shown is from cell types manufactured in 1974 and 1975.

[4] G.F.J. Garlick and D.R. Lillington, "Design Study of Large Area 8x8 cm Wrapthrough Cells for Space Station," *Space Photovoltaic Research and Technology 1986, NASA CP-2475*, pp. 87-97 (1987).

[5] L.W. Slifer, Jr., "The Goddard SFC High Efficiency Cell Development and Evaluation Program," *Solar Cell High Efficiency and Radiation Damage, NASA CP-2020*, pp. 7-23 (1977).

[6] H. Bebermeier, "Design and Qualification of BSR- Solar Cells for Future Solar Arrays," *Proc. 14th IEEE Photovoltaic Specialists Conf.*, pp. 1144-1147 (1980).

[7] M.A. Green, A.W. Blakers, and C.R. Osterwald, "Characterization of High-Efficiency Silicon Solar Cells," *J. Appl. Phys. 58* (11), pp. 4402-4408 (1985).

[8] B. Anspaugh, Jet Propulsion Laboratories, private communication, Mar. 1992; data set 10-11 Oct. 1990 RSW.

[9] I. Weinberg, C.K. Swartz, R.E. Hart, and R.L. Statler, *Radiation and Temperature Effects in GaAs, InP, and Si Solar Cells, NASA Technical Memorandum 89870*, presented at the 19th IEEE Photovoltaic Specialists Conference, 1987.

[10] R. Cross, J. Burrage, C. Hardingham and A, Potts, "GaAs Space Solar Cells Pilot Production Experience...," *Proc. European Space Power Conference, ESA SP-294, Vol. 2*, Oct. 1989, pp. 525-529.

[11] C.K. Swartz and R.E. Hart Jr., "Temperature and Intensity Dependence of the Performance of an Electron Irradiated (AlGa)As/GaAs Solar Cell," *Solar Cell High Efficiency and Radiation Damage - 1979, NASA CP-2097* pp. 217-226 (1979).

[12] E. Fanetti, G. Fiorito, and C. Flores, "Concentration and Temperature Performances of GaAs-GaAlAs Solar Cells", *Proc. 2nd EC Photovoltaic Solar Energy Conf.*, Berlin, April 1979, 447-454.

[13] G.H. Walker, E.J. Conway, K.H. Hong and J.H. Heinbockel, "High Temperature Properties of GaAlAs/GaAs Heteroface Solar Cells," *Proc. 14th IEEE Photovoltaic Specialists Conf.*, pp. 1098-1101 (1980).

[14] C.R. Osterwald, T. Glatfelter and J. Burdick, "Comparison of the Temperature Coefficients of the Basic I-V Parameters for Various Types of Solar Cells," *Proc. 19th IEEE Photovoltaic Specialists Conf.*, pp. 188-193 (1987).

[15] I. Weinberg, C.K. Swartz and R.E. Hart, "Performance and Temperature Dependencies of Proton Irradiated n/p and p/n GaAs and n/p Si Cells," *Proc. 18th IEEE Photovoltaic Specialists Conference*, 344-349 (1985).

[16] I. Weinberg, *et al.*, "Comparative Radiation Resistance, Temperature Coefficient and Performance of..." *Solar Cells, Vol. 22*, pp. 113-123 (1987). Data from table 4 corrected to 28°C.

[17] R.J. Walters, R.L. Statler, and G.P. Summers, "Temperature Coefficients and Radiation Induced DLTS Spectra of MO-CVD Grown n+p InP Solar Cells," *Space Photovoltaic Research and Technology 1991, NASA CP-3121*, May 1991, 42-1.

[18] R. Venkatasubramanian *et al.*, "High Temperature Performance and Radiation Resistance of High Efficiency Ge and Si(0.07)Ge(0.93) Solar Cells on Lightweight Ge Substrates," *Proc. 22nd IEEE Photovoltaic Specialists Conf., Vol. 1,* pp. 85-89 (1991)

[19] J. Boswell, B. Anspaugh and R. Mueller, "Thin Film Photovoltaic Development at Phillips Laboratory," *Proc. 23rd IEEE Photovoltaic Specialists Conference,* 1324-1329 (1993).

[20] R.M. Burgess, W.E. Devaney and W.S. Chen, "Performance Analysis of CIS and GaAs Solar Cells Aboard the LIPS-III Flight Boeing Lightweight Panel," *Proc. 23rd IEEE Photovoltaic Specialists Conference,* 1465-1468 (1993).

[21] C.R. Osterwald, "Translation of Device Performance Measurements to Reference Conditions," *Solar Cells, Vol. 18,* pp. 269-279 (1986).

[22] E.L. Ralph and E.J. Stofel, *Advanced Hardened Array, Vol. I, Preliminary Design, WRDC-TR-90-2098,* Nov. 1990, pp. 156-182.

[23] S. Wojtczuk *et al.*, "Monolithic Two-terminal GaAs/Ge Tandem Space Concentrator Cells,"*Proc. 22nd IEEE Photovoltaic Specialists Conf., Vol. 1,* pp. 73-79 (1991).

[24] J.C.C. Fan, Theoretical Temperature Dependence of Solar Cell Parameters, *Solar Cells 17,* 309-315 (1986).

[25] L. Gerlach, "HST Solar Generator Electrical Performance During the First Year in Orbit," *Proc. European Space Power Conference, ESA SP-320,* Aug. 1991, pp. 725-731.

[26] P.A. Iles and S. Khemthong, "The Alpha Factor: Controlling Solar Cell Absorptance," *Proc. 13th IEEE Photovoltaic Specialists Conf.,* pp. 327-332 (1978).

[27] F. Reissman and M. Baumgart, "Application of Gallium Arsenide Solar Cell Arrays for Long Duration Low Earth Orbit Missions Like Columbus," *Proc. European Space Power Conference, ESA SP-294,* Vol. 2, Oct. 1989, pp. 525-529.

[28] TRW, *Advanced Photovoltaic Solar Array Design Final Technical Report CDRL-008,* 3 November 1986, JPL Contract 957358, p. 3-65 to 4-69.

[29] S. Khemthong, P. Iles, M. Roberts, C. Karnopp and N. Senk, "Performance of Large Area, Thin Silicon Cells," *Proc. 20th IEEE Photovoltaic Specialists Conf., Vol. 2,* pp. 960-963 (1988).

[30] M. Uesuegi *et al.*, "High Efficiency Silicon Solar Cells for Space Use," *Proc. 22nd IEEE Photovoltaic Specialists Conf., Vol. 2,* pp. 1521-1524 (1991).

[31] G.F. Virshup, B-C Chung, and D. Brinker, "Temperature Coefficients of Multijunction Solar Cells," *Proc. 21st IEEE Photovoltaic Specialists Conf.,* pp. 336-338 (1991).

[32] H.S. Rauschenbach, *Solar Cell Array Design Handbook,* Van Nostrand Reinhold Company New York, 1980, "Solar Cell Performance Data," pp. 196-241.

[33] H.B. Curtis and R.E. Hart, Jr., "Temperature Coefficients for Concentrator Cells at Various Electron and Proton Fluence Levels", paper 889048, Intersociety Energy Conversion Engineering Conference 1988, 85-89.

[34] R. Loo and G.S. Kamath, *High Efficiency GaAs Concentrator Cells,* Report Final report HAC REF F4356 for NASA Lewis Research Center, contract NAS3-23877, p. 5-7, Mar. 1988.

[35] L. Fraas *et al.*, *Optoelectronics Devices and Technologies, Vol. 5,* No. 2, 297-310 (1990).

[36] M.W. Wanlass, T.J. Coutts, J.S. Ward, and K.A. Emery, "High-Efficiency Heteroepitaxial InP Solar Cells," *Proc. 22nd IEEE Photovoltaic Specialists Conf., Vol. 1,* pp. 159-165 (1991).

[37] N. Takata, *et al*, "Space Proven GaAs Solar Cells - Main Power Generation for CS-3," *Proc. 21st IEEE Photovoltaic Specialists Conf., Vol. 2*, pp. 1219-1225 (1990).

[38] S.P. Tobin *et al.*, "High Efficiency GaAs/Ge Monolithic Tandem Solar Cells," *Proc. 20th IEEE Photovoltaic Specialists Conf., Vol. 1*, pp. 405-410 (1988).

[39] R.J. Lammert, "Characteristics of Solar Cells at Low Temperatures," *Proc. 7th IEEE Photovoltaic Specialists Conference*, 97-100 (1968).

[40] C.H. Liebert, "Solar Cell Performance at Jupiter Temperature and Solar Intensity," *Proc. 7th IEEE Photovoltaic Specialists Conference*, pp. 92-96 (1968).

[41] IEEE, session 2B, "Temperature-Illumination Studies," *Proc. 8th IEEE Photovoltaic Specialists Conference*, pp. 110-168 (1970)

[42] Y. Ichikawa, "Large-Area Amorphous Silicon Solar Cells With High Stabilized Efficiency," *Proc. 23rd IEEE Photovoltaic Specialists Conf.*, pp. 27-33 (1993).

[43] K. Mullaney *et al.*, "Infra-Red Reflective Coverglasses: the Next Generation," *Proc. 23rd IEEE Photovoltaic Specialists Conf.*, pp. 1363-1368 (1993).

[44] W.T. Beauchamp, T.T. Hart and M.L. Sanders, "Blue/Red Reflecting Solar Cell Covers for GaAs Cells," *Proc. 23rd IEEE Photovoltaic Specialists Conf.*, pp. 1487-1490 (1993).

[45] G.A. Landis, "Satellite Eclipse Power by Laser Illumination" (paper IAF-90-053), *Acta Astronautica, Vol. 25* No. 4, 229-233 (1991).

[46] G.A. Landis, "Space Power by Ground-based Laser Illumination," *IEEE Aerospace and Electronics Systems, Vol. 6* No. 6, 3-7, Nov. 1991; presented at 26th Intersociety Energy Conversion Engineering Conf., Aug. 1991, *Vol. 1*, pp. 1-6.

[47] G.A. Landis, "Photovoltaic Receivers for Laser Beamed Power," *Journal of Propulsion and Power, Vol. 9* No. 1, 105-112 (1993); presented at *22nd IEEE Photovoltaic Specialists Conference*, Las Vegas NV, Oct. 1991, *Vol. II*, 1494-1502.

[48] D. Wilt, N. Fatemi, R. Hoffman, P. Jenkins, D. Brinker, D. Scheiman, R. Lowe, D. Chubb, M. Faur, and F. DeAngelo, "High Efficiency, Low Bandgap InGaAs PV Device Development for TPV Power Systems," *13th Space Photovoltaic Research and Technology Conference*, NASA Lewis, June 14-16 1994 (proceedings in press).